



## Platinum nanoflowers decorated three-dimensional graphene–carbon nanotubes hybrid with enhanced electrocatalytic activity

Rajesh <sup>a,c,\*</sup>, Rajat K. Paul <sup>b,1</sup>, Ashok Mulchandani <sup>a,\*</sup>

<sup>a</sup> Department of Chemical and Environmental Engineering, University of California, Riverside, CA 92521, USA

<sup>b</sup> Department of Mechanical Engineering, University of California, Riverside, CA 92521, USA

<sup>c</sup> Polymer & Soft materials Section, CSIR-National Physical Laboratory, Dr. K.S. Krishnan Road, New Delhi-110012, India

### HIGHLIGHTS

- One-step CVD process for the synthesis of 3D-carbon electrode as Pt catalyst support.
- 3D electrode comprises bamboo like MWNTs on single layer graphene film (G-MWNTs).
- Platinum nanoparticles are electrochemically deposited over G-MWNTs hybrid.
- Pt/G-MWNTs hybrid exhibited enhanced catalytic performance towards methanol oxidation.

### ARTICLE INFO

#### Article history:

Received 19 June 2012

Received in revised form

29 August 2012

Accepted 30 August 2012

Available online 7 September 2012

#### Keywords:

Graphene

Carbon nanotubes

Pt nanoparticles

Electrochemical activity

Methanol oxidation

### ABSTRACT

A three-dimensional carbon electrode, in the form of vertically grown multiwalled carbon nanotubes (MWNTs) on a single layer graphene floor (G-MWNTs) is synthesized by one-step chemical vapor deposition (CVD) method, as supporting material for platinum (Pt) electrocatalyst. Nanostructured Pt catalyst is electrodeposited onto this 3D-carbon electrode and their structural and electrochemical properties are investigated by transmission electron microscopy (TEM), scanning electron microscopy (SEM), energy dispersive spectroscopy (EDS), cyclic voltammetry (CV) and electrochemical impedance spectroscopy. The electrocatalytic performance of the modified electrode (Pt/G-MWNTs) towards methanol oxidation is also investigated by CV. Experimental results demonstrate an enhanced efficiency of the G-MWNTs hybrid film, as Pt catalyst support, for methanol oxidation in comparison to pristine single layer graphene electrode with regard to electroactive surface area, forward anodic peak current density, onset oxidation potential, diffusion efficiency and the ratio of forward to backward anodic peak current density ( $I_f/I_b$ ). This enhanced electrochemical and catalytic performance towards methanol oxidation is attributed to the high surface area of three-dimensional G-MWNTs hybrid film due to synergistic combination of both structural and electrical properties of 2D-graphene and 1D-MWNTs, allowing higher dispersion of Pt.

© 2012 Elsevier B.V. All rights reserved.

## 1. Introduction

Nanostructured carbon materials because of their electrical conductivity and ability to improve catalytic activity in fuel cells, has been receiving a great deal of interest [1–3]. Many types of carbon, including carbon black, carbon nanofibers and carbon nanotubes have been used as support materials for catalysts in fuel cell systems. The CNTs have excellent intrinsic properties such as

their unique morphology including inherent size and hollow geometry, high electrical conductivity and good chemical stability that make them promising supports materials for heterogeneous catalysts [4]. There is an increasing demand for growing CNTs directly on the substrate to minimize the contact resistance between the CNTs and conducting substrate.

The recent emergence of graphene, a one-atom thick planar sheet of hexagonally arrayed  $sp^2$  carbon atoms, due to its unique physicochemical properties: high specific surface area (theoretically  $2630\text{ m}^2\text{ g}^{-1}$  for single-layer), excellent electrical conductivity, large surface area per unit volume and stability, has opened a new opportunity for utilizing this 2D carbon material as a heterogeneous catalyst support in fuel cells [5–7]. Platinum nanoparticles supported on 2D-structure graphene when applied as electrocatalyst for

\* Corresponding authors. Polymer & Soft materials Section, CSIR-National Physical Laboratory, Dr. K.S. Krishnan Road, New Delhi-110012, India. Tel.: +91 951 827 5696.

E-mail addresses: [rajesh\\_csir@yahoo.com](mailto:rajesh_csir@yahoo.com) (Rajesh), [adani@engr.ucr.edu](mailto:adani@engr.ucr.edu) (A. Mulchandani).

<sup>1</sup> These authors contributed equally to this work.

electrochemical oxygen reduction reactions and methanol oxidation in fuel cells exhibited a higher catalytic activity and less susceptibility to carbon monoxide poisoning when compared to Pt supported on carbon black [8]. However, the excellent properties of graphene emerge only in the planar direction. On-the-other-hand, in carbon nanotubes (CNTs) these properties emerge in the axial direction while providing high specific surface area, current density and thermal conductivity. Thus, a graphene–CNT hybrid which combines the unique properties of the two carbon allotropes in all directions and provides a high surface area per unit volume for increased catalyst loading could be an ideal electrode material for fuel cells.

Recently, syntheses of graphene–CNT hybrid were reported. Methods included combining graphene and CNT by solution processing, solid-phase layer stacking of CNT film on graphene film or chemical vapor deposition (CVD) [9–13]. Amongst the various methods reported, CVD [13] has following advantages: a) a large area can be synthesized in a facile single-step process, b) CNTs are connected to the large-area graphene floor which can enable the ballistic transport of charge carriers through 1D CNTs and their collection through the high carrier mobility 2D graphene floor and c) provide high surface-to-volume ratio to achieve enhanced current density.

On the one hand, significant efforts have been made to synthesize high-surface-area graphene-based composites as electrode materials to achieve high catalytic activity. On the other hand, synthesis of noble electrocatalyst nanoparticles with uniform size and good dispersion over the carbon supports, as an electrocatalytic material also remained to be a demanding work. With the development of nanotechnology, nanostructured materials offers new avenues for searching and designing effective electrocatalysts, which have attracted attention of many researchers and advances the progress in this field. Among the nanocatalysts, platinum based electrocatalysts are exclusively utilized for catalyzing oxygen reduction reaction (ORR) and methanol oxidation reaction (MOR) in Direct Methanol Fuel Cells (DMFCs) [14]. However, several limitations such as high cost, low availability of platinum and irreversible inactivation of the catalysts by CO-poisoning species limit the widespread commercialization of DMFCs. It is therefore required to develop low cost catalyst systems with comparable activity towards methanol oxidation reaction and better CO-tolerance for DMFCs. For example in direct methanol fuel cells (DMFCs), depositing platinum loaded carbon material films on conducting substrates is a crucial step in the construction of electrodes. Drop casting [15], electrophoretic [16] and electrostatic layer-by-layer methods have been reported for the deposition of Pt–CNT film on the conducting substrates [17] for applications to DMFCs. However, there are some critical factors that limit the particular application of methanol fuel cell, including sluggish kinetics of methanol oxidation at anode leading to high over-potentials and the high cost of noble Pt-based catalysts. Therefore, the development of support material with high surface area is of considerable interest to effectively disperse catalyst particles and to reduce the catalyst loading with enhancing the catalytic activity for the electrooxidation of methanol.

We report the fabrication, characterization and electrocatalytical activity of a platinum nanoparticles decorated unique large-area three-dimensional carbon electrode comprising of multiwalled carbon nanotubes (MWNTs) vertically grown on a single layer graphene (G-MWNTs) floor by one step CVD method. Comparative studies were carried out for structural, electrochemical and electrocatalytical performance in terms of MOR for the developed G-MWNTs hybrid supported Pt catalyst with respect to electro-deposited Platinum nanoparticles on pristine graphene electrode.

## 2. Experimental

### 2.1. Chemicals

Electrocatalyst precursor salts, i.e.,  $H_2PtCl_6 \cdot 6H_2O$  and  $RuCl_3$ , were purchased from Sigma. All other chemicals were of analytical grade and used as received without further purification. Double distilled water was used through all experiments.

### 2.2. Methods

Graphene was grown by acetylene ( $C_2H_2$ )-chemical vapor deposition (CVD) process on a copper foil ( $\sim 2.54\text{ cm}^2$ ). For G-MWNTs film growth, copper foil was decorated with 1 nm thick iron nanoparticles using an e-beam evaporator (Temescal, BJD-1800). The iron nanoparticles and Cu foil acted as catalysts for MWNTs growth and graphene, respectively. The growth substrates were placed inside a fused silica tube (5 cm inside diameter by 100 cm long) and the temperature raised to 750 °C, under flowing  $Ar/H_2$ , 100 sccm (standard cubic centimeter per min)/50 sccm, atmosphere. A 50 sccm flow of  $C_2H_2$  was supplied for 10 min in the tube once the temperature stabilized at 750 °C. After the growth process, the MFC for  $C_2H_2$  was turned off, followed by cooling the furnace to room temperature in flowing  $Ar/H_2$  atmosphere. Graphene film formed on the backside of the Cu foil was removed by  $O_2$  plasma, followed by etching of the Cu foil in a 1 M aqueous  $FeCl_3$  solution to collect single layer graphene and/or G-MWNTs film grown on the other side. Subsequent cleaning of the films was performed with an aqueous HCl (5%) and deionized (D.I.) water for several times to remove iron particles from the hybrid as well as etching solution. The complete removal of Cu and Fe was necessary as they had been considered as membrane contaminants in DMFCs. GC electrodes (3 mm diameter) were polished first with emery paper and then with aqueous slurries of fine alumina powder (1 and 0.05 μm) on a polishing cloth, and finally rinsed with D.I. water in an ultrasonic bath for 5 min, then dried with a high-purity  $N_2$  stream. Single layer graphene and G-MWNTs hybrid films were transferred over GCE, followed by drying at 50 °C temperature for 1 h in oven to obtain the graphene/GCE and G-MWNTs/GCE electrodes, respectively. Pt nanoparticles were electrochemically deposited onto the G-MWNTs hybrid film modified GCE and single layer graphene modified GCE by potential sweeping of 25 cycles each between +0.30 and –0.70 V, at a scan rate of 50 mV s<sup>-1</sup>, in 0.1 M HCl solution containing 5 mM  $H_2PtCl_6 \cdot 6H_2O$ , under identical experimental conditions. The Pt/G-MWNTs/GCE and Pt/graphene/GCE so obtained were washed with D.I. water and dried at 50 °C temperature for 30 min, in oven, under vacuum. RuPt/G-MWNTs/GCE was prepared from an equimolar solution mixture of 0.25 M each  $H_2PtCl_6 \cdot 6H_2O$  and  $RuCl_3$  in a cyclic voltammetry mode with 25 potential cycles between the same potential window, under identical conditions, as mentioned above for Pt deposition. All the experiments were carried out at room temperature. The amount of Pt deposited on the Pt/G-MWNTs/GCE and Pt/graphene/GCE was calculated from the charge consumed (the overall charge that passed during the cathodic sweeps of potential) during the electrodeposition of Pt by using Faraday's law, considering a value of 4 for  $n$  according to the following faradic reaction (Eq. (1)):



So, the quantity of deposited Pt ( $m_{Pt}$ ) is obtained from Eq. (2):

$$m_{Pt} = Q_{Pt} \cdot M / 4F \quad (2)$$

where  $M$  is the atomic weight of Pt (195.09 g mol $^{-1}$ ), and  $F$  is the Faraday constant (96,485.309 C mol $^{-1}$ ). Based on charge consumed, the mass of electrodeposited platinum on the G-MWNT hybrid and graphene film was found to be 332  $\mu\text{g cm}^{-2}$  and 357  $\mu\text{g cm}^{-2}$ , respectively.

### 2.3. Instrumentations

Detailed materials characterization of the synthesized films was performed using transmission electron microscopy (TEM; Philips, CM300, Japan), scanning electron microscopy (SEM; Leo, 1550) and Energy dispersion spectroscopy (EDS; Leo, 1550). Electrochemical characterization was performed with a CHI 750C (CH instruments Inc., USA). A three electrode system was employed, while the Pt nanoparticles modified electrode (Pt/G-MWNTs/GCE or Pt/graphene/GCE) was the working electrode, Ag/AgCl with KCl solution acted as the reference electrode, and the platinum wire was the counter electrode. All cyclic voltammetric measurements were performed for at least three cycles, until a reliable and repeatable response was achieved and data presented were taken from the 3rd cycle.

## 3. Results and discussion

### 3.1. Morphological and electrochemical characterization

Pt was electrochemically deposited on the surface of three-dimensional carbon electrode of vertically grown multiwalled carbon nanotubes (MWNTs) on a single layer graphene floor (G-MWNTs) as described in the experimental section; the resulting

morphologies of the carbon materials before and after Pt deposition are shown in (Figs. 1 and 2).

Scanning electron microscopy (SEM) and transmission electron microscopy (TEM) studies were employed to investigate the morphology of as prepared G-MWNTs hybrid film. As shown in the SEM image (Fig. 1a), the one-step G-MWNTs synthesis method produced a highly dense MWNTs of an average tube diameter of 30 nm growing uniformly over the entire large-area graphene surface. A low magnification TEM image of G-MWNTs hybrid film transferred on a lacey carbon-supported Cu TEM grid (Fig. 1b) depicts growth of MWNTs from graphene surface. In the 1 nm Fe nanoparticles decorated Cu substrate, Fe and Cu were acting as metal catalysts for MWNT and graphene growth, respectively, during the one-step CVD growth process at 750 °C in flowing Ar (100 sccm)/H<sub>2</sub> (50 sccm)/C<sub>2</sub>H<sub>2</sub> (20 sccm) atmosphere. In the unique catalyst system of Fe decorated Cu substrate, the MWNTs growth was made possible by typical vapor–liquid–solid (VLS) mechanism, whereas the graphene growth occurred by surface catalysis mechanism. After completing the growth of the single layer graphene and G-MWNT hybrid, these materials were separated as a film with the complete etching of Cu foil in 1 M FeCl<sub>3</sub> solution. The floating films so obtained were washed off repeatedly with 5% HCl followed by D.I. water to remove the residual impurities of Cu and Fe particles. On the other hand, a TEM grid having G-MWNTs transferred on it, were placed upside down to clearly observe the interface between the MWNTs and graphene floor. In the bottom view of G-MWNTs hybrid film (Fig. 1c), the individual MWNT's root had seamless crystalline contact with the graphene floor showing hollow circular pattern (as shown with dotted circles) comprising

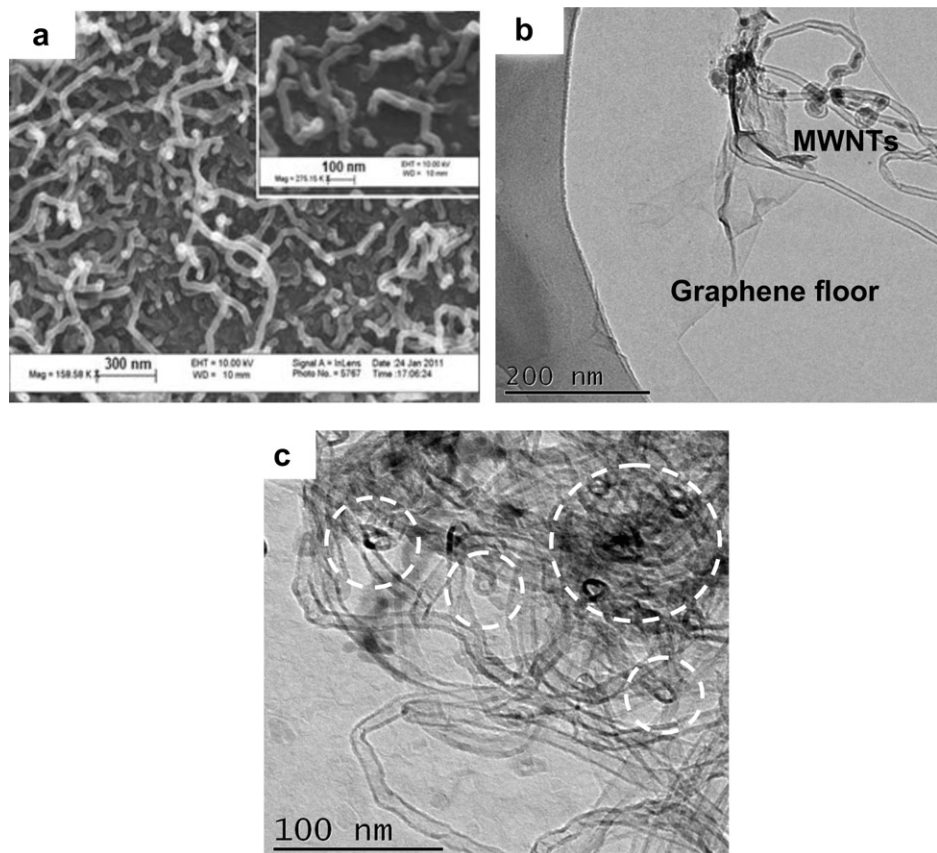


**Fig. 1.** SEM and TEM images of the G-MWNTs hybrid film. (a) SEM image of G-MWNTs film composed of vertically grown MWNTs on graphene floor, covering the GCE electrode, (b) TEM image of MWNTs growth from graphene surface and (c) TEM image of bottom view of G-MWNTs hybrid film showing crystalline contact between individual MWNT's root (dashed circles) and the graphene surface.

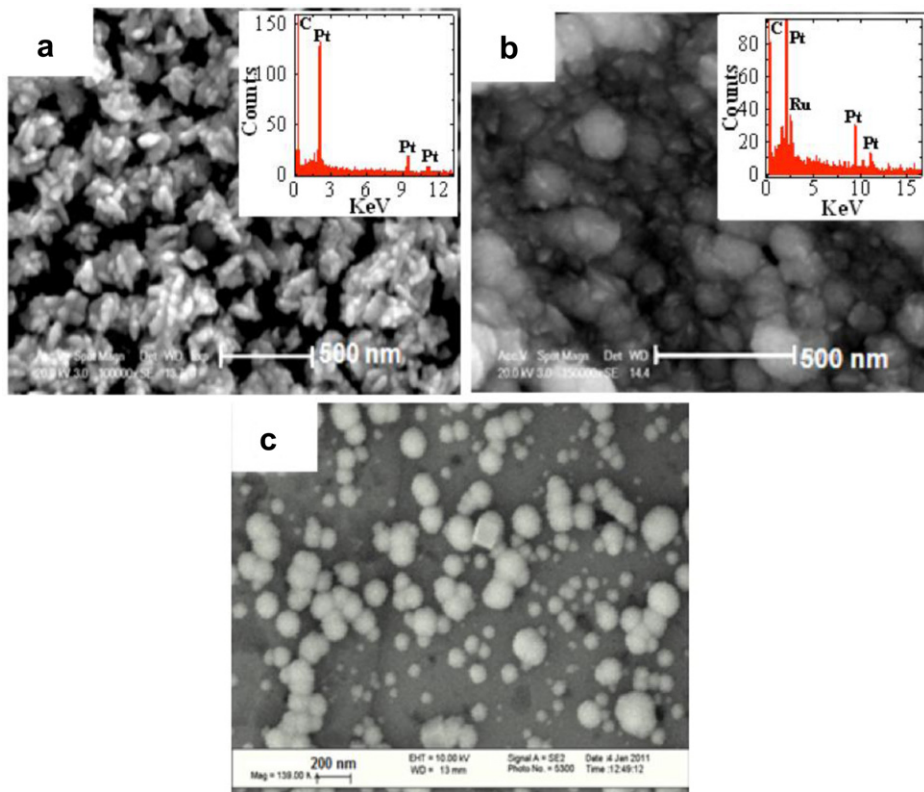


**Fig. 2.** SEM images of (a) Pt/G-MWNTs (inset shows EDS pattern), (b) RuPt/G-MWNTs (inset shows EDS pattern) and (c) Pt/graphene.

of typical C–C covalent bond between the two carbon allotropes. This crystalline contact between MWNTs and graphene would remarkably reduce the contact resistance to achieve maximum charge transfer through the G-MWNTs hybrid system, as was established earlier through measurement of *I*–*V* curves showing Ohmic contact between the CNT pillars and graphene film [18].

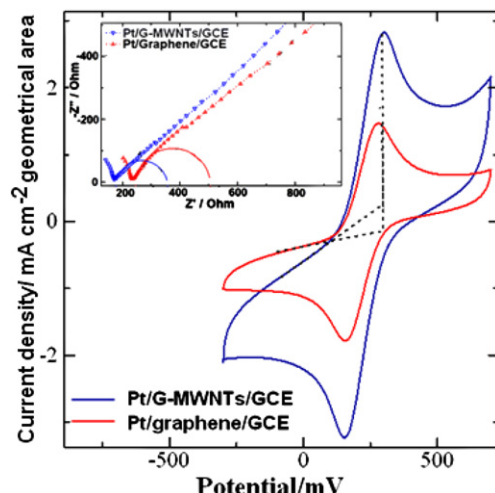
Fig. 2a and b show SEM micrograph and EDS profiles (insets) of G-MWNTs after electrodeposition of Pt and RuPt nanoparticles, respectively. As evident from the images, the electrodeposition conditions employed in this work produced a uniformly distributed flower-like structure comprising clusters of needles/flakes with needle size of 60–90 nm in case of Pt alone, and a combination of both spherical and needle like bimetallic particles in the case of RuPt, over the G-MWNTs hybrid film producing a high surface-to-volume catalyst. In comparison, identical electrodeposition conditions employed on monolith graphene resulted in Pt nanoparticles ranging from 20 to 200 nm diameters having a few aggregated clusters of particles spread out on the graphene film (Fig. 2c) surface.

Fig. 3 shows the cyclic voltammetry (CV) with electrochemical impedance spectra (insets of Fig. 3) of Pt/G-MWNTs/GCE and Pt/graphene/GCE electrodes in degassed 0.01 M  $K_3[Fe(CN)_6]$ /0.1 M KCl solution in deionized water at a scan rate of 50 mV s<sup>-1</sup>. Well-defined oxidation and reduction peaks were observed with significant difference in peak-to-peak potentials separation on these electrodes. The high peak current density was noticed on the Pt/G-MWNTs/GCE electrode, indicating the highest electroactive surface area. The electroactive surface area of the electrodes were calculated using the Randles–Sevcik equation [19]

$$I_p = 2.69 \times 10^5 A D^{1/2} n^{3/2} v^{1/2} c \quad (3)$$

where  $n$  (=1) is the number of electrons participating in the redox reaction,  $A$  is the electroactive surface area ( $\text{cm}^2$ ),  $D$  (=  $6.70 \times 10^{-6}$

$\text{cm}^2 \text{s}^{-1}$ ) is the diffusion coefficient of  $Fe(CN)_6^{3-}$  in solution,  $c$  (=0.01 M) corresponds to the concentration of the redox probe ( $K_3[Fe(CN)_6]$ ), and  $v$  is the scan rate of the potential perturbation ( $\text{V s}^{-1}$ ). The electroactive surface area for Pt/G-MWNTs and Pt/Graphene electrodes were found to be 1.21 and 0.074  $\text{cm}^2$ , respectively (Table 1), showing a 16 times larger surface area for Pt/GMWNTs as compared to Pt/graphene. In accordance with the inverse relationship with the electroactive surface area, a low value of charge transfer resistance ( $R_{ct}$ ) was observed in impedance spectra for Pt/G-MWNTs in comparison to Pt/graphene (Table 1). Correspondingly,



**Fig. 3.** Cyclic voltammograms of Pt/G-MWNTs/GCE and Pt/graphene/GCE (inset: EIS spectra) in 0.01 M  $[Fe(CN)_6]^{3-/-4-}$  + 0.1 M KCl in degassed water, at scan rate of 50 mV s<sup>-1</sup>.

**Table 1**

Comparison of different electrochemical and MOR performance between Pt/graphene, Pt/G-MWNTs and RuPt/G-MWNTs hybrids.

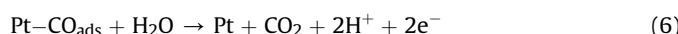
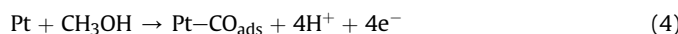
Electrode	EA (cm <sup>2</sup> )	R <sub>ct</sub> (Ohm cm <sup>2</sup> )	K <sup>0</sup> <sub>app</sub> (cm s <sup>-1</sup> )	I <sub>f</sub> /I <sub>b</sub>	I <sub>f</sub> * (mA cm <sup>-2</sup> )	Mass activity* (mA mg <sub>Pt</sub> <sup>-1</sup> )	E <sub>onset</sub> (V)
Pt/graphene	0.074	18.74	1.41 × 10 <sup>-3</sup>	1.65	8.36	23.41	0.41
Pt/G-MWNTs	0.121	12.75	2.08 × 10 <sup>-3</sup>	1.11	42.31	127.43	0.27
RuPt/G-MWNTs	—	—	—	9.38	—	—	0.22

EA = electroactive area of the electrode, R<sub>ct</sub> = surface specific charge transfer resistance, K<sup>0</sup><sub>app</sub> = apparent electron transfer rate constant for Fe (CN)<sub>6</sub><sup>3-/4-</sup>, C = specific capacitance, I<sub>f</sub> = forward oxidation current density, I<sub>b</sub> = backward anodic current density, I<sub>f</sub>\* = 3.0 M methanol forward oxidation current density, E<sub>onset</sub> = onset oxidation potential.

the heterogeneous electron transfer rate constant, K<sup>0</sup><sub>app</sub> (=RT/n<sup>2</sup>F<sup>2</sup>CR<sub>ct</sub>), which is directly proportional to electroactive surface area, showed a higher value for Pt/G-MWNTs than Pt/graphene (Table 1). These results are in conformity with the pattern observed in CV measurements, confirming the highest electroactive surface area for Pt/G-MWNTs. The low electroactive area and sluggish electron transfer rate for the Pt/graphene is attributed to a perfectly crystalline nature (negligible defects) of the single layer graphene film, as reported recently by electrochemical measurement on pristine epitaxial graphene grown on silicon carbide (SiC) surface [20].

### 3.2. Methanol electro-oxidation

The electrocatalytic activities of Pt/G-MWNTs and Pt/graphene were further investigated and compared towards the oxidation of methanol, which is directly related to applications in DMFCs. Fig. 4a shows typical cyclic voltammograms for the electro-oxidation of different methanol concentrations in 0.1 M H<sub>2</sub>SO<sub>4</sub> at Pt/G-MWNTs. CV profile for Pt/graphene is presented in Supplementary Information (Fig. S1). All CV profiles consisted of two strong anodic peaks, a forward peak and a backward peak, which are well known to originate from the electro-oxidation of methanol and the intermediate, respectively. The forward and backward anodic peaks in the scan correspond to oxidation of methanol forming Pt-adsorbed CO, that is known to poison the electrocatalyst, and CO<sub>2</sub> (Eqs. (4) and (5)) and the oxidation of adsorbed carbonaceous species to CO<sub>2</sub> (Eq. (6)), respectively [21].



Additionally, the Fig. 4b illustrate that the methanol oxidation current density increased with increasing methanol concentrations up to 3 M at the Pt/G-MWNTs but leveled at 2 M at the Pt/graphene electrode. This phenomenon is ascribed to the saturation of active sites at the electrode surface. Further, the methanol oxidation current density was highest at Pt/G-MWNTs at all methanol concentrations. Pt loading has direct effect on the oxidation of methanol. Hence, to compare the performance of these two different electrodes same number of CV cycles, 25 in this study, was used for Pt nanoparticles deposition on both G-MWNTs and graphene electrodes.

This number of CV cycles value was chosen based on our observation and that beyond 25 CV cycles, the Pt nanoparticles starts getting aggregated and results in the formation of a thin film of Pt. The electrochemical Pt deposition is an effective procedure in comparison to the chemical route, which involves complex fabrication steps and also the presence of impurity might be involved during preparation. The MOR performance of these two electrodes was compared by comparing their corresponding mass activity towards methanol oxidation by normalizing the forward oxidation current density to mass of the electrodeposited Pt. The mass activity of the Pt/G-MWNT was found to be 127.43 mA mg<sub>Pt</sub><sup>-1</sup>, which is about 5 times higher than that of 23.41 mA mg<sub>Pt</sub><sup>-1</sup> obtained with graphene for 3.0 M methanol oxidation in 0.1 M H<sub>2</sub>SO<sub>4</sub> at a scan rate of 50 mV s<sup>-1</sup>. This significant increase in the mass activity with the G-MWNT methanol oxidation is due to the controlled uniform electrodeposition of the Pt, due to higher 3D surface area of the electrode. The mass activity of 102.12 mA mg<sub>Pt</sub><sup>-1</sup> with G-MWNT hybrid was found to be higher than 60 mA mg<sub>Pt</sub><sup>-1</sup> with commercial (E-TEK) Pt/C and comparable to 82.6–146.4 mA mg<sub>Pt</sub><sup>-1</sup> for Pt/CNTs [22] for 2.0 M methanol oxidation, which may be further increased by decreasing the Pt loading and reducing the particle size by controlling the Pt electrodeposition on the electrode surface.

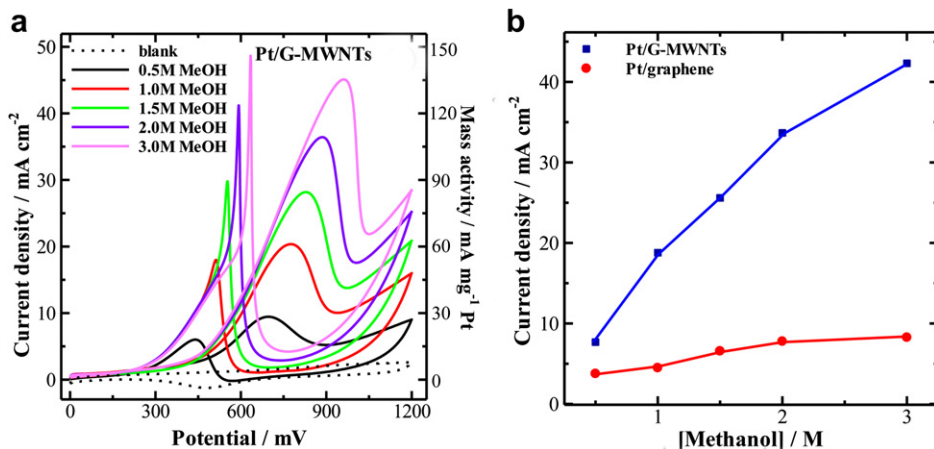
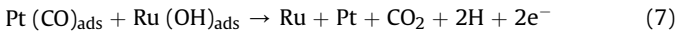


**Fig. 4.** Cyclic voltammograms with the current density normalized to the geometrical surface area (left) and the mass activity (right) of (a) Pt/G-MWNTs in 0.0–3.0 M CH<sub>3</sub>OH/0.1 M H<sub>2</sub>SO<sub>4</sub> at scan rate of 50 mV s<sup>-1</sup> and (b) plot of forward anodic peak current density vs. CH<sub>3</sub>OH concentration for Pt/G-MWNTs and Pt/graphene.

Although a good catalytic activity was observed at Pt/G-MWNTs, poisoning of Pt by the carbonaceous intermediate, CO in particular, on the electrode surface cannot be overlooked. RuPt is commonly accepted as best electrocatalyst for methanol oxidation. Bimetallic Ru and Pt was electrochemically deposited on G-MWNTs, under identical conditions as described for Pt deposited electrodes, and evaluated for methanol oxidation. As shown in Fig. 6b, the backward anodic current peak was significantly reduced at RuPt/G-MWNTs when compared to Pt alone (Fig. 5a) in 1.0 M CH<sub>3</sub>OH/0.1 M H<sub>2</sub>SO<sub>4</sub>, indicating the removal of CO<sub>ads</sub> by Ru via the following (Eq. (7)) bi-functional mechanism [23].



The ratio of the forward peak current density ( $I_f$ ) to backward anodic peak current density ( $I_b$ ), used to describe the catalyst tolerance to carbonaceous species accumulation, were observed to be 9.38, 1.11 and 1.65 for RuPt/G-MWNTs, Pt/G-MWNTs and Pt/graphene, respectively. Although the  $I_f/I_b$  at Pt/G-MWNTs (1.11) is significantly lower than Pt/graphene, it is higher than those of recently reported for Pt/graphene oxide (0.83) and Pt/MWNT (0.72) [24] and comparable to commercial Pt/carbon black (1.27) from Johnson Matthey [7]. Furthermore, the  $I_f/I_b$  for RuPt/G-MWNTs (9.38) is more than two-fold higher than that for commercial Pt/carbon black (4.39) from Johnson Matthey [7]. The approximately 9-fold higher  $I_f/I_b$  for RuPt/G-MWNTs over Pt/G-MWNTs confirms the ability of the bimetallic catalyst to withstand poisoning from carbonaceous materials by oxidizing them to CO<sub>2</sub>.

The onset potential ( $E_{\text{onset}}$ ) of methanol oxidation is also an indicator for determining and comparing the electrocatalyst activity for methanol oxidation [25]. The  $E_{\text{onset}}$  (Fig. 5 insets) was found to be in the order of RuPt/G-MWNTs (0.22 V) < Pt/G-MWNTs (0.27 V) < Pt/graphene (0.41 V), revealing that G-MWNTs supported catalyst, both Pt and RuPt, had enhanced electrocatalysis capability in the methanol oxidation when compared to graphene catalyst support. In comparison, commercial Pt/C (E-TEK), Pt/carbon black (Johnson Matthey) and RuPt/carbon black (Johnson Matthey) had significantly higher onset potential values of 0.55 V, 0.797 V and 0.597 V, respectively [7,22].

Kinetics of methanol oxidation reaction at Pt deposited electrodes was investigated by studying the relationship between the forward anodic peak current density of methanol oxidation and CV scan rate ( $v$ ). Fig. S2 shows CV curves for methanol oxidation at Pt/G-MWNTs and Pt/graphene, at a scan rate of 25–125 mV s<sup>-1</sup>. A

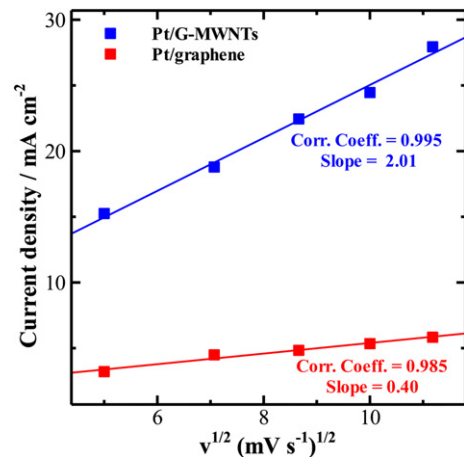


**Fig. 6.** Relationship of anodic forward peak current density vs. scan rate for Pt/G-MWNTs/GCE and Pt/graphene/GCE.

linear relationship between forward peak current density and  $v^{1/2}$  for Pt/G-MWNTs and Pt/graphene, shown in Fig. 6, suggests that the oxidation behavior of methanol at both electrodes is controlled by diffusion process [26]. The larger slope for Pt/G-MWNTs (2.01) compared to Pt/graphene (0.40) is indicative of a fast diffusion process of methanol on the surface of G-MWNTs hybrid film than those of graphene catalyst supports. This result is also attributed to large surface area of Pt nanoparticles catalyst per unit geometrical area of G-MWNTs hybrid electrode and is consistent with SEM and electroactive surface measurement studies, further suggests G-MWNTs hybrid film to be promising catalyst support for the direct DMFCs applications.

#### 4. Conclusions

We have demonstrated an efficient fabrication of Pt nanoparticles deposited unique three-dimensional carbon electrode system called G-MWNTs as catalyst support for the electro-oxidation of methanol. SEM analysis confirmed that flower-like Pt nanostructures of about 60–90 nm in size with cluster of needles were electrochemically deposited over the entire hybrid nanostructure. On the basis of mass specific activity the Pt/GMWNT exhibited the highest MOR performance and fast diffusion process as compared to graphene supported Pt catalyst. Additionally, RuPt/

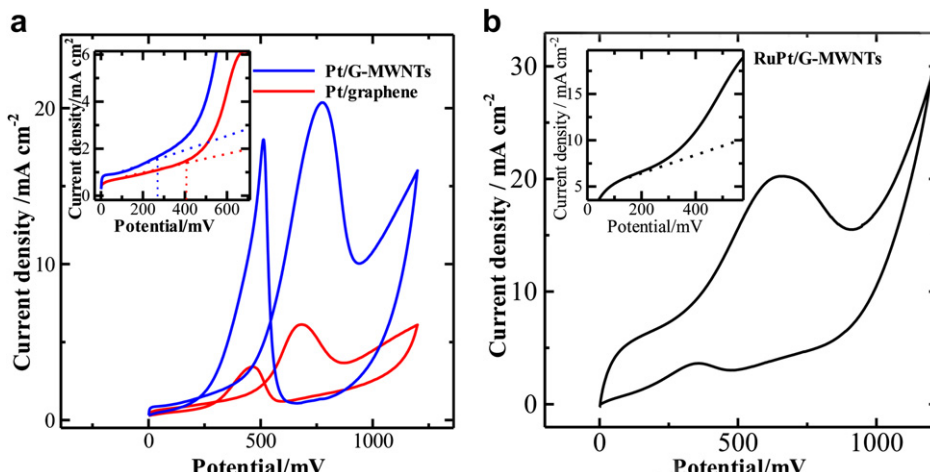


**Fig. 5.** Electrocatalytic performance of (a) Pt/G-MWNTs/GCE and (b) RuPt/G-MWNTs/GCE in 1 M CH<sub>3</sub>OH/0.1 M H<sub>2</sub>SO<sub>4</sub> at a scan rate of 50 mV s<sup>-1</sup>.

G-MWNTs prepared in the present work reduced the backward anodic current peak significantly by oxidizing the carbonaceous intermediate to CO<sub>2</sub>. The high performance of G-MWNTs as catalyst support for electro-oxidation of methanol is due to the large surface area of unique 3D carbon nanostructure having efficient charge transfer at G-MWNTs/electrolyte interface allowing higher dispersion of Pt, and good electrical properties of MWNTs. This MOR performance may further be improved by better controlling the Pt nanoparticle size with optimizing the electrodeposition process. These results suggest that G-MWNTs could be a potential candidate as a catalyst support material for the applications in DMF fuel cells.

## Acknowledgements

We acknowledge the Bourns College of Engineering Dean and Nanosense Inc. for financial support. Rajesh is thankful to Indo-US Science & Technology Forum (IUSSTF), New Delhi, India for providing a research fellowship.

## Appendix A. Supporting information

Supporting information related to this article can be found at <http://dx.doi.org/10.1016/j.jpowsour.2012.08.088>.

## References

- [1] E.J. Yoo, T. Okada, T. Kizuka, J. Nakamura, *J. Power Sources* 180 (2008) 221–226.
- [2] J. Prabhuram, T.S. Zhao, Z.K. Tang, R. Chen, Z.X. Liang, *J. Phys. Chem. B* 110 (2006) 5245–5252.
- [3] S. Liao, K.A. Holmes, H. Tsapralis, V.I. Briss, *J. Am. Chem. Soc.* 128 (2006) 3504–3505.
- [4] G.G. Wildgoose, C.E. Banks, R.G. Compton, *Small* 2 (2006) 182–193.
- [5] C. Xu, X. Wang, J.W. Zhu, *J. Phys. Chem. C* 112 (2008) 19841–19845.
- [6] Y.C. Si, E.T. Samulski, *Chem. Mater.* 20 (2008) 6792–6797.
- [7] E.J. Yoo, T. Okada, T. Akita, M. Kohyama, J. Nakamura, I. Honma, *Nano Lett.* 9 (2009) 2255–2259.
- [8] L. Qu, Y. Liu, J.-B. Baek, L. Dai, *ACS Nano* 4 (2010) 1321–1326.
- [9] D. Yu, L. Dai, *J. Phys. Chem. Lett.* 1 (2010) 467–470.
- [10] V. Tung, L.M. Chen, M.J. Allen, J.K. Wassei, K. Nelson, R.B. Kaner, Y. Yang, *Nano Lett.* 9 (2009) 1949–1955.
- [11] Z.J. Fan, J. Yan, L.J. Zhi, Q. Zhang, T. Wei, J. Feng, M.L. Zhang, W.Z. Qian, F. Wei, *Adv. Mater.* 22 (2010) 3723–3728.
- [12] C.Y. Li, Z. Li, H.W. Zhu, K.L. Wang, J.Q. Wei, X. Li, P. Sun, H. Zhang, D.J. Wu, *J. Phys. Chem. C* 114 (2010) 14008–14012.
- [13] X.C. Dong, B. Li, A. Wei, X.H. Cao, M.B. Chan-Park, H. Zhang, L.J. Li, W. Huang, P. Chen, *Carbon* 49 (2011) 2944–2949.
- [14] B.C.H. Steele, A. Heinzel, *Nature* 414 (2001) 345–352.
- [15] G. Girishkumar, T.D. Hall, K. Vinodgopal, P.V. Kamat, *J. Phys. Chem. B* 110 (2006) 107–114.
- [16] Y. Xing, *J. Phys. Chem. B* 108 (2004) 19255–19259.
- [17] J. Yuan, Z. Wang, Y. Zhang, Y.F. Shen, D. Han, Q. Zhang, X. Xu, L. Niu, *Thin Solid Film* 516 (2008) 6531–6535.
- [18] R.K. Paul, M. Ghazinejad, M. Penchev, J. Lin, M. Ozkan, C.S. Ozkan, *Small* 6 (2010) 2309–2313.
- [19] Q. Wan, X. Wang, F. Yu, X. Wang, N. Yang, *J. Appl. Electrochem* 39 (2009) 1145–1151.
- [20] C.X. Lim, H.Y. Hoh, P.K. Ang, K.P. Loh, *Anal. Chem.* 82 (2010) 7387–7393.
- [21] C.H. Chen, K. Shimizu, Y.Y. Lin, F. Bailey, I.F. Cheng, C.M. Wai, *Energy Fuels* 21 (2007) 2268–2271.
- [22] M.S. Saha, R. Li, X. Sun, *J. Power Source* 177 (2008) 314–322.
- [23] V. Selvaraj, M. Alagar, *Electrochem. Commun.* 9 (2007) 1145–1153.
- [24] Y. Li, W. Gao, L. Ci, C. Wang, P.M. Ajayan, *Carbon* 48 (2010) 1124–1130.
- [25] D.M. Han, Z.P. Guo, Z.W. Zhao, Y.Z. Meng, D. Shu, H.K. Liu, *J. Power Sources* 184 (2008) 361–369.
- [26] K. Honda, M. Yoshimura, T.N. Rao, D.A. Tryk, A. Fujishima, K. Yasui, Y. Sakamoto, K. Nishio, H. Masuda, *J. Electroanal. Chem.* 514 (2001) 35–50.